Earth Surf. Dynam. Discuss., 1, 855–889, 2013
www.earth-surf-dynam-discuss.net/1/855/2013/
doi:10.5194/esurfd-1-855-2013

Earth **Surface** Dynamics
Discussions
Open Access

Assessing the natural morphological sensitivity of a pinned, soft-cliff, sandy coast to a changing wave climate

A. Barkwith[1], C. W. Thomas[1], P. W. Limber[2,*], M. A. Ellis[1], and A. B. Murray[2]

[1]British Geological Survey, Keyworth, Nottingham, NG12 5GG, UK
[2]Nicholas School of the Environment, Duke University, Durham, NC, USA
[*]now at: Dept. of Geological Sciences, University of Florida, Gainesville, FL, USA

Received: 23 September 2013 – Accepted: 29 October 2013 – Published: 19 November 2013

Correspondence to: A. Barkwith (andr3@bgs.ac.uk)

Published by Copernicus Publications on behalf of the European Geosciences Union.

Abstract

The impact of future sea level rise on coastal erosion as a result of a changing climate has been studied in detail over the past decade. The potential impact of a changing wave climate on erosion rates, however, is not typically considered. We explore the effect of changing wave climates on a pinned, soft-cliff, sandy coastline, using as an example the Holderness coast of East Yorkshire, UK.

The initial phase of the study concentrates on calibrating a model to recently measured erosion rates for the Holderness coast using an ensemble of geomorphological and shoreface parameters under an observed offshore wave climate. Stochastic wave climate data are perturbed gradually to assess the sensitivity of the coastal morphology to changing wave climate. Forward-modelled simulations indicate the nature of the morphological response of the coast to changes in wave climate over the next century. Results indicate that changes to erosion rates over the next century will be spatially and temporally heterogeneous, with a variability of up to ±25 % in the erosion rate relative to projections under constant wave climate. The heterogeneity results from the current coastal morphology and the sediment transport dynamics consequent on differing wave climate regimes.

1 Introduction

The coastal zone and immediate hinterland is a highly important socio-political domain (Pendleton, 2010). It is also amongst the most vulnerable, particularly when climate change alters sea level, weather systems and wave climates. Understanding the geomorphological response and sensitivity of coastal regions to changes in sea level, weather patterns and wave climates are thus key society-relevant scientific inquiries. Many studies have focused on observation and monitoring, in order to understand the key processes and the rates at which they happen, particularly with regard to erosion or accretion along low-lying "soft" coasts dominated by weakly or unconsolidated sediments. Numerical modelling, parameterised in part by observational data, is increasingly used to study both coastal processes and the response of coastal evolution to climatic changes, under current conditions and those which might pertain in the future.

In this paper, we report a numerical modelling study of a soft-cliff, sandy coastline, which is pinned in place at the updrift end by a rocky headland that resists erosion. We use the Holderness Coast, eastern England as an example (Fig. 1). Whilst well-studied and monitored (Montreuil and Bullard, 2012; Scott Wilson, 2009; Quinn et al., 2009), the possible future states of this coastline have received only minimal investigation using numerical modelling (Castedo et al., 2012). Efforts to understand this coastline are vital as it is among the most rapidly eroding of coastlines in Europe, with concomitant and serious threats to people, property, economy and infrastructure along its length. Valentin (1971) and de Boer (1964) showed that shoreline retreat at Holderness has been on the order of kilometres since the sea reclaimed the North Sea Basin at the end of the Quaternary. Many ancient settlements recorded in texts, such as the 12th Century Domesday Book and old maps, have been lost to the sea and current settlements and infrastructure continue to be lost, damaged or under imminent threat as the coastline retreats westwards. On the human level, loss of land and property can often be catastrophically rapid because of the episodic nature of cliff collapse over short time-scales.

In order to understand the mechanisms and retreat rates within the Holderness littoral cell, and to develop practical coastal management strategy (see Scott Wilson, 2009), most recent studies have focussed on monitoring and measurement of coastline position and beach profiles over several years (Brown et al., 2012; Montreuil and Bullard, 2012; Quinn et al., 2009). Modern observational techniques often use rapid LIDAR scanning systems to provide accurate measurements of cliff retreat and volume loss. Many datasets of coastal change now exist to support coastal management decisions. However, such studies do not necessarily reflect what will happen in the future. The relatively short time-scales over which these studies have been made inevitably represent only recent “snap-shots” of geomorphological processes. Such geomorphological processes are stochastic and therefore short records may not represent long term averaged conditions. These studies also have limited predictive value, especially if the factors that control coastline evolution change significantly in the coming decades. Mesoscale modelling can allow long-term behavioural trends to be identified and explore the role of changes in driving forces. In addition, numerical modelling can be used to understand the morphological sensitivity of the Holderness Coast under different climate change scenarios. Through modelling, the impact of such changes on settlements, land and infrastructure in the longer term can be assessed, even if only to show that current coastal recession, both in rate and form, is likely to continue in the forthcoming decades.

In order to investigate how a pinned, soft-cliff, sandy coastline might respond to future changes in hydrodynamic driving processes, and the rates at which such changes may occur, we have applied a modified numerical coastline evolution model (Ashton & Murray, 2006a, b; Ashton et al., 2001) to the Holderness coast. The model allows us to postulate how spatially and temporally sensitive the Holderness coastline is to differing wave climate scenarios. Changes to wave height or approach angle modify gradients in alongshore transport, determining beach volume flux rates and subsequently cliff erosion rates. Previous work has shown that changing the distribution of wave-approach angles can change the shape of a sandy coastline (McNamara et al., 2011; Slott et al., 2006); here we investigate how wave climate change scenarios could affect a soft-cliff coastline.

2 Geomorphology and wave climate of the Holderness coastline

2.1 Geomorphology

The Holderness coast stretches ~ 60 km from chalk cliffs at Flamborough Head in the north to Spurn Head in the south (Scott Wilson, 2009; Quinn et al., 2009). The coastline is cut mainly in glacial till deposited during Devensian glaciations (c. 35 to 11.5 ka BP).

Cliffs range from 2 to 35 m in height. The glacial till is heterolithic clay, sand and gravel resting on a chalk platform sloping gently to the east (Catt, 2007). Coastal defences, including groynes, rock revetments and concrete sea walls protect the larger towns and villages along the coastline. Recent recession rates, ranging between c. 1 $\mathrm{m\,yr^{-1}}$ and c. 5 $\mathrm{m\,yr^{-1}}$ depending on time and location, have been documented by Quinn et al. (2009) and Montreuil and Bullard (2012). South of Flamborough Head, wave-driven cliff erosion has created one of the fastest retreating coastlines in Europe (IECS, 1994). With little external sediment transported into the Holderness coastline from the north (May, 1980), material derived from eroded cliffs supply the bulk of the sediment flux southwards along the coastline. The Humber estuary forms the southern boundary of the sediment cell, acting as a sink for sediment transported along the coast. The narrow sand and gravel spit at Spurn Head extends southwestwards across the mouth of the Humber for 3.5 km, and is known to have complex dynamics (Ciavola, 1997).

2.2 Current wave climate

The current wave climate off the Holderness coast is recorded by the Hornsea Directional Waverider III Buoy (CCO, 2013). This buoy has recordeed mean half-hourly significant wave height, period and direction since June 2008. Wave climate is characterised by northeasterly wave approach (Fig. 2), with a mean period of 7.3 s (2.6 to 18.8 s) and a seasonally variable significant wave height (0.2 to 3.5 m) with an annual mean of 0.9 m.

Daily-averaged data for the years 2009 and 2010 (used for this study) are shown in Fig. 2. The dominant NNE mode exhibits frequency percents between 16 and 25 %. This mode was particularly strong in 2010. In 2009 modes from the ENE and ESE were more prominent. The differences in wave directions between the two years will be reflected in the modelled sediment fluxes and resultant coastline evolution. Significant wave heights were higher more frequently in 2010 than in 2009 (Fig. 2). The data show that seas off Holderness were rougher and more focussed in direction during 2010, and thus likely to cause more erosion and sediment transport than in 2009. A generally monotonic decline in wave period, as the wave direction rotates clockwise from north (0°), can be observered in the buoy data (Fig. 2). The distribution of wave period with wave direction is similar for both 2009 and 2010, although the greater spread in wave direction is evident in the 2009 data. Wave periods lie in largely the same range in both years; between 4 s and 14 s. On a few days, offshore waves, derived from the SW, have periods in the 8 to 14 s range. The longest period waves are mainly derived from the northeasterly direction, the dominant mode in wave direction. We infer these waves to be the long period swell waves derived from North Atlantic low pressure systems tracking across the northeast Atlantic, the waves refracting round northern Britain and down the North Sea. For just a few days each year, there are long period waves travelling from a southwesterly direction.

2.3 Future wave climate

Possible future wave climates for the North Sea have been studied in detail over the last decade, the motivation being to examine the effects of climate change on coastal flooding (Grabemann and Weisse, 2008; Woth et al., 2006) and ocean infrestructure (Wang et al., 2004).

Oceanic modes can increase or decrease the strength of incoming winds over Europe and have a dominant effect on the wave climate. For Europe, the North Atlantic Oscillation (NAO) is the dominant mode, modifying the path of the prevailing westerly winds and the position of storm tracks with a quasi-decadal frequency (Hurrell and van Loon, 1997; Hurrell, 1995). The NAO, and subsequently the intensity, frequency and tracks of storms, are likely to be effected by changes in climate over the coming century (Woollings et al., 2010). This is currently being studied using a multi-system modelling approach; greenhouse gas emission scenarios are used to force global circulation and regional climate models (IPCC, 2007), producing the atmospheric variables (wind speeds and direction) needed in the derivation of wave climate using a wave model. The impact of future climate states on the NAO have not been quantified with any degree of certainty (Woollings, 2010); the triggering mechanisms for phase switching, oceanic-atmospheric interactions that drive the system and teleconnections with other systems, are poorly understood (Bladé et al., 2012).

Insufficient knowledge of the NAO combined with the range of greenhouse gas predictions and the variety of models used for research has produced a wide range of possible perturbations to future wind patterns and hence to future wave climates. Sutherland and Wolf (2002) linked a wave climate model to a coupled global climate model and found that predicted wave height changes are within ±5 % of current significant wave height. Due to the uncertainties inherent in the modelling, Hulme et al. (2002) provide a qualitative assessment of future wave climates in the Atlantic, suggesting modifications to the NAO would produce more westerly wave directions, therefore reducing wave height in the North Sea basin. Further study by DEFRA (2010) on the impacts of climate change on wave climate highlights an increase in North Sea wave heights between 1973 and the mid-1990s, though more recent trends are unclear. Future UK wave climate projections were found to be very sensitive to the climate model scenarios for storms, which themselves are uncertain (DEFRA, 2010).

Due to the uncertainty in the prediction of North Sea wave climate, two years (2009–10) of measured wave climate were use to drive the model, cycling sequentially over the two year period. In the calibration and baseline simulations, these data were not perturbed. In subsequent runs, the wave direction data were rotated, as a whole, by angles of between 0 and 20° in clockwise and counter-clockwise directions, selected at random for each run. Similarly, significant wave heights were perturbed by up to ±0.4 m. Further details are given in Sect. 4.

3 Modelling

Previous simulations of Holderness coastal morphology have focussed on cliff stability modelling at sub-centennial timescales. These studies employ two dimensional cross-section models to consider rotational (for example, Quinn et al., 2010; Gibbons, 2004) and translational (Robertson, 1990) cliff failure, with cliff topple as the prime coastal recession mechanism for the latter. Castedo et al. (2012) combine these failure mechanisms with the hydrodynamics and geotechnical characteristics of the coast determined at several locations, using observed recession rates to calibrate parameters. Future erosion rates at each location were calculated for the remainder of this century and found to have a quasi-linear response to sea-level rise. Potential changes in wave climate and their possible impact on the evolution of coastal morphology and retreat into the future have not been investigated. Two dimensional planform models of coastal morphology allow the influence of wave climate variability on erosion and accretion rates along the coast to be explored. This section describes the model used in this study and its underlying conceptual framework.

We have adapted the coastline evolution model originally developed by Ashton et al. (2001), Ashton and Murray (2006a, b), and Valvo et al. (2006) to allow sediment inputs derived from cliff retreat (Fig. 3). Wave-generated erosion of a sea cliff may be spatially and temporally variable on short time scales (i.e., focused at the cliff toe, causing undercutting and subsequent overhang collapse; Young and Ashford, 2008), however over decadal the scale, cliff retreat can be treated as a process considered to occur evenly over the entire cliff profile (Limber and Murray, 2011a; Walkden and Hall, 2005). The rate of cliff retreat is thus time-averaged, and implicitly includes shorter-term changes such as storm-induced erosion (Sallenger et al., 2002). For simplicity, the model cliff topography is uniform, reflecting the mean cliff height of the Holderness coast.

Beach geometry and rates of sandy shoreline change are also averaged over short-term events (List et al., 2006). As the shoreline position changes, beach geometry remains constant, sediment is spread over the entire beach profile, and bathymetry contours are shore-parallel (Ashton and Murray, 2006a). The change in sandy coastline position η_b) through time is governed by;

$$\frac{\partial \eta_b}{\partial t} = -(1-\gamma HC)\frac{\mathrm{d}\eta_c}{\mathrm{d}t} + S - \left(\frac{1}{D}\frac{\partial Q_\mathrm{S}}{\partial x}\right), \tag{1}$$

where γ is a beach geometry constant that converts the volume of material eroded from the sea-cliff into a beach width; H is sea-cliff height divided by the depth to which the beach extends; C is the proportion of sea-cliff material that is coarse enough to contribute to beach width (Limber et al., 2008); S is a beach sediment loss rate; D is the water depth (closure depth) to which shore-parallel bathymetry contours extend; Q_s is alongshore sediment transport (Ashton and Murray, 2006a); and x is alongshore position.

Equation (1) is discretised into uniform cells. The first term on the right-hand side represents sediment input into the coastal system as cliffs erode and rock is weathered into mobile sediment. There is an additional cliff retreat rate term (η_c) because the beach is pinned to the cliff as it retreats landward. The beach acts as a protective cover, reducing wave impact at the cliff toe. Accordingly cliff retreat rate is highest when local beach width (w) at a particular location is zero, decreasing exponentially as beach width increases (Lee, 2008; Valvo et al., 2006; Sallenger et al., 2002). To represent wave energy attenuation as waves refract towards the coastline (Adams et al., 2002), cliff retreat rate also depends on the mean daily breaking wave angle. The flux of coastal wave energy is maximized when waves approach a model cell orthogonally, and decreases as the incident wave angle increases. Cliff retreat through time is thus a function of wave angle and beach width, and is calculated by;

$$\frac{\mathrm{d}\eta_c}{\mathrm{d}t} = \cos(\phi - \theta)\mathrm{Er}_0 e^{-\frac{w(t)}{w_\mathrm{scale}}}, \tag{2}$$

where ϕ is the incident angle of the deep-water wave, θ is the orientation of the coastline for a particular model cell, Er_0 is the time-averaged, bare-rock cliff retreat rate, and w_scale is a length scale constant that depends on the beach width that provides near complete cover from wave attack, so that cliff retreat becomes negligible (i.e. ~ 1 % of the maximum value; Limber and Murray, 2011b; Sallenger et al., 2002). Different lithologies can be represented in the model by varying Er_0 and C: Er_0 represents erosional resistance, and C reflects the fraction of fine grade sediment in the fallen material. More resistant lithologies (the chalk at Flambrough Head) have a lower Er_0 than rocks more suseptable to erosion (the glacial till along the Holderness embayment). Through a calibration process (described in Sect. 4), site-specific, uniform values for Er_0 and C can be set using long-term field observations of cliff retreat (e.g. Hapke and Reid, 2007). Although the model does not explicitly model the smaller-scale structural variations that affect the retreat rate of the rock, such as joints and fractures (Dickson et al., 2004; Trenhaile et al., 1998; Clark and Johnson, 1995), the long-term cliff retreat rate allows implicit representation (e.g., structurally weaker rocks will have higher rates of retreat). This assumes a relatively even distribution of these features within a given rock type over a given spatial scale.

The second term in Eq. (1) represents constant beach sediment losses (S) due to the attrition and subsequent offshore transport of beach sediment in the surf zone, or as a human impact, such as sand mining (Perg et al., 2003; Thornton et al., 2006; Limber and Murray, 2011a, b).

The final term represents the gradient in wave-driven alongshore sediment flux that causes large-scale and long-term shoreline change (erosion, accretion, the formation of capes and spits). Sediment flux is calculated via the common Coastal Engineering Research Center (CERC) sediment transport equation, as discussed at length elsewhere (van den Berg et al., 2012; List and Ashton, 2007; Valvo et al., 2006; Ashton and Murray, 2006a, b; Ashton et al., 2001; Komar, 1971). The magnitude of sediment flux is a function of incoming wave angle relative to the orientation of the coastline, and sediment transport occurs at a greater rate when wave height and period (through effects on shoaling and refraction) increase. Therefore, wave climate characteristics will have a marked effect on how sediment is distributed along a coastline and ultimately how large-scale coastline morphology will evolve.

A factor not expressed within Eq. (1) is the wave shadowing by salient sectors of coast updrift or downdrift of the sector of interest, for example where headlands occur. The area covered by the shadowed zone is dependent on the incoming angle of the wave, with respect to the shoreline, and the size of the salient. In the shadow, it is assumed that there is no sediment transport when waves impinge beyond the critical angle at which shadowing occurs; however, sediment can be transported into this zone when waves approach at angles for which there is no shadowing (Ashton and Murray, 2006a).

In the original model, offshore water wave climate is represented by a fixed offshore wave height and period, and by a four-bin probability density function (PDF), which defines the degree of asymmetry in wave direction and the fraction of high angle waves (see Ashton et al., 2001). Recent wave climate records are available for the North Sea, off the coast of the Holderness cell, allowing a truer representation of current wave climate. The model was therefore adapted to use observed wave records to drive the simulation.

For this study, the observed wave climate consisted of a daily average significant wave height, period and direction. Waves that propergated in an offshore direction, as determined by the average orientation of the coast, were converted to a null wave angle and height so that no sediment was transported during that timestep. As the simulated periods were much longer than the period covered by current wave data, the model wave climate was cycled for the duration of the run. To account for mesoscale (decadal to centennial) changes in wave climate, linear adjustments to wave height, period and angle were applied.

4 Calibration and setup

The model is discretised into 100 m square cells, representing the region from Flamborough Head in the north to the Humber Estuary in the south, and a daily timestep used to drive the model. The eastern boundary is approximately 40 km east of Hull and the western boundary 20 km to the west. The northern and southern boundaries of the model contain a mixture of nodes representing land, beach and sea, and use a specified boundary condition that allows a sand flux out of, but not into, the system. The western (land) and eastern (sea) boundaries are set with a no-flow condition such that sediment can not be created, removed or passed through these interfaces. The Humber Estuary is represented as a sediment sink in the model. In reality, the Humber River transports sediment into the North Sea basin, an area outside the model domain. For the purpose of this study we ignore the spit at Spurn Head and this region is therefore excluded from both the calibration process and data analysis.

Lithological and shoreface properties have been measured at several locations along the Holderness coastline (Newsham et al., 2002). These observations are spatially limited and are not likely to represent the coastline of the littoral cell as a whole. To derive coastline average lithological and shoreface components with which to populate the model, we calibrated coastline recession rates over the past 15 yr to the observed rates compiled by Montreuil and Bullard (2012), using a stochastic approach. To improve the root mean square error (RMSE) between simulated and observed rates, larger coastal defences were represented in the simulation as slow eroding surfaces.

A Monte Carlo approach (Metropolis and Ulam, 1949; Robert and Casella, 2004) consisting of 2,000 members was used for the calibration, with the ensemble representing a range of lithological and shoreface properties. Each member was allocated ten years of spin-up time, enough for each member to reach a steady-state condition, before the fifteen years of simulation. The attenuation of steady-state ensures that beach sediment, which is initialised as uniform along the coast, is distributed and that any small-scale roughness in the DEM used to initialise the coastline shape can be removed. The coastal erosion rate at each node was determined and the RMSE calculated for each member of the ensemble, based on the observed rates. Following calibration, the closest simulated match to the observed data has an RMSE of 13.20 m and a mean error of 0.81 m (Fig. 4). The agreement between simulated and observed erosional rates is spatially variable along the coast. In the simulation we assume a homogeneous geology and topography, and consequently the coastline has a relatively uniform retreat rate around the designated coastal defences identified in the model.

The uniform retreat exhibited by the simulated coast is not apparent in reality. This difference is attributable to factors that may be considered either temporal or spatial. Temporally, the measured retreat rate reflects short-lived events such as storms and sand-bar placement, whereas the simulated retreat is averaged. Spatially, the susceptibility of the coastline to erosion is treated homogeneously in the model (apart from the division into hard and soft rock), whereas in reality, the geology is heterogeneous and many small-scale man-made coastal defences are interspersed along the length of the coast. This heterogeneity is composed of regions more (due to joints and stream heads) and less (due to higher cohesion or hard coastal defences) susceptible to erosion. Erosional homogeneity is also affected by cliff failure and the subsequent protection this affords the new cliff face. These processes can be considered as implicit in the model if the process occurs evenly along the coast.

The input parameters for the ensemble member with the lowest RMSE were used to initialise the future coastal sensitivity simulations up to 2100. Through comparison of future simulations to a baseline, run with the recently recorded unperturbed wave data, changes to the coastal morphology and the sensitivity of coastline to change are appraised. To assess the sensitivity of the coastline to possible future wave climates, an ensemble of 1350 model runs was undertaken, with wave climate parameters rotated by up to $\pm 20^\circ$ and significant wave height changed by up to ± 0.4 m. Modifications to wave climate used in individual ensemble members are linear over the ninety year period from 2010 to 2100. Changes in wave direction and significant wave height were selected at random between the bound levels for each of the simulations, with the initial state represented by the recently observed wave climate data.

The model domain, grid spacing and time-step are identical to the calibration setup. To ensure the model was initialised from a steady-state, a ten year spin-up phase (as assessed during the calibration), starting from the current coastline position under current wave conditions, was performed before each simulation was undertaken. The output from the spin-up period is omitted from the results and analysis; erosion rates and sensitivity to wave climates are presented and discussed with reference to the start date 1st January 2010.

5 Results and analysis

The simulated distribution of absolute erosion along the coast by 2100 for the ensemble of wave climate perturbations is presented in Fig. 5a. Zero erosion represents the initial coastline position for 2010, and positive values represent a westward coastal retreat. Landward retreat was near zero at Flamborough Head and increase to a maximum of 150 m in central sections of the coast. Toward the south, total erosion reduces in a quasi-linear fashion to 145 m at Easington (far right in the plot). Within the near-linear changes in coastline position, there is little range in the absolute erosion produced by the ensemble. The largest range in absolute erosion occurs at between 10 km and 30 km south of the northern domain boundary, where the difference between the 10th and 90th percentiles is around 60 m. When compared with the 2010 baseline (Fig. 5b) the results reveal that future erosion rates could either accelerate or slow depending on the nature of the wave climate change. The negative skewing of the relative erosion implies that a reduction in erosion rate for the coast as a whole is more likely, although relative erosion along the coast is highly heterogeneous (Fig. 5b). The southern region (defined as south of the sea wall at Hornsea, Fig. 1) shows little variation in relative erosion, and the 50th percentile is close to zero. As with the absolute erosion rates, the northern region (defined as north and including the sea wall at Hornsea, Fig. 1) exhibits the greatest range in relative ensemble erosion rates over the ninety year period. The first to third quartiles also show a wide range of values in this region, indicating a spread of retreat values throughout the ensemble. Depending on the wave climate attributes of the ensemble member, there is up to ±30 m (~ 25 %) disparity in erosion relative to the baseline.

By spatially averaging the relative change in erosion for each ensemble member, erosion can be represented by a single value, allowing an assessment of the individual and combined influences of rotating wave direction and perturbed wave height. Figure 6a shows that the relationship between the change in wave direction and relative erosion is linear within the range -20° to 0°, with counter-clockwise rotation progressively reducing relative erosion. Clockwise rotations in the wave climate of up to 18° increase erosion rates, although unlike the counter-clockwise trend, the trend is non-linear. There is further asymmetry between clockwise and counter-clockwise rotations where, under certain circumstances, clockwise rotations greater than 18° can lead to a reduction in erosion. The influence of a changing wave height on relative erosion is presented in Fig. 6b. It reveals a weak relationship, where reduction in relative erosion occurs with an increasing wave height. This relationship is clearest at the limit of reduced erosion rates, which are present at only the most negative rotations. At this limit, mean relative erosion was reduced by up to 8 m at a wave height perturbation of −0.4 m, and by 13 m under a positive wave height perturbation of 0.4 m.

The range in relative erosion for a particular wave height or rotation is partially controlled by the corresponding perturbation. For example, the range of relative erosion determined at a rotation of −10° is a function of the range of wave heights. This suggests that both wave parameters influence relative erosion, although the strongest control remains wave rotation as this generates the smallest range in relative erosional for any particular rotation value. To highlight the relationship between relative erosion and perturbations in wave height and rotation, they are plotted together in Fig. 6c and d. As highlighted in the previous plots, a clockwise rotation results in increased relative erosion and a counter-clockwise rotation less relative erosion. The small, subtle effects of changing wave height are also highlighted: for any particular rotation, the relative erosion rate decreases by a small amount as wave height increases. These relationships are altered under the most extreme clockwise changes under wave rotations (above 18^{o}), where greater wave heights increase relative erosional.

The northern and southern regions of the coastline respond differently to changes in wave climate. To assess these differences, the relative change in erosion for each region is presented in a spatially averaged form (Figs. 7 and 8). In the northern region, there appears to be a highly linear coupling between rotation and erosion, even under clockwise rotations. The reduction in relative erosion, apparent at the extreme of clockwise rotation for some ensemble members where the whole coastline is considered (see Fig. 6), is not apparent in the northern region. For this region there is no definitive relationship between changing wave height and relative erosion. In the south, maximum relative erosion occurs at clockwise rotations of around 8°. In comparison to the north, the range of relative erosion is lower in the south, suggesting a balance in the height and rotation perturbations. The relationship between increasing wave height and relative erosion reduction is broadly linear in the south. This relationship produces a weak gradient under small rotations, but with large clockwise rotations the gradient in increased. This trait is highlighted in Fig. 8, where, for the southern region, there is a relatively strong horizontal gradient in relative erosion at clockwise wave rotations above 18°.

By plotting the average relative erosion against time, arising temporal divergences were elucidated (Fig. 9). Throughout the simulation, the average relative erosion rate remains near zero. Over the first 40 yr of simulation, the range of possible erosion rates also shows little asymmetry, indicating a low tendency for either increased or decreased erosion rates. Modifications to the wave climate over this period were small, as the wave climate perturbations were applied linearly to the baseline climate for each scenario. As the wave factors begin to impart a larger influence, there is a non-linear response from the system. The range between both the outliers and the 25th and 75th percentiles get progressively larger. The data becomes negatively skewed, implying that a reduction in relative erosion is more likely given the input parameters of the ensemble.

6 Discussion

The erosional response to a modified wave climate for a pinned, soft-cliff, sandy coastline has been assessed in this study. The following discussion highlights three overarching impacts of morphology on recession that may be extrapolated to similar coastlines. Detail is provided for the Holderness coast, however separate analysis would be required to determine the same level of detail for a different coastline of similar morphology.

The response of the Holderness coastline, to modified wave climates is spatially heterogeneous, with different sections of the coastline exhibiting variable rates of erosion under differing wave climate scenarios. In the north, clockwise rotations increase relative erosion and counter-clockwise rotations reduce erosion. In the south, increased relative erosion peaks occur at a clockwise rotation of about 5°. The range in spatially averaged relative erosion between ±10° spans 18 m for the north and 7 m for the south. This difference in sensitivity for the northern and southern sections of the model is due to a combination of factors. Firstly, the angle between that of the wave direction and the coast increases towards the south as the coastline orientation changes. Secondly, there is a heterogeneous distribution of beach sediment through time and space, and hence variable protection from erosion, along the coast. Thirdly, the CEM accounts for shadowing of the coast by salients. Thus, Flamborough Head shadows the north and protects this region from erosion under certain wave climates.

6.1 Shoreline angle

The dominant observed wave direction is approximately 030°. This results in angles with the coastline of between 90° and 20° in the north region and a constant 20° in the south. Modelled sediment transport is greatest when offshore waves impinge the coast at relative angles of between 30° and 50°, depending on the equation used for breaking-wave-driven, alongshore sediment transport (Ashton and Murray, 2006a). For the CERC equation, maximum sediment transport occurs at 42°. Parts of the coastline within the northern region are orientated relatively close to this angle, with respect to the dominant wave direction, and therefore show the greatest response to a changing dominant wave orientation. The variation in coastline orientation with respect to the incoming wave direction creates a gradient in transport, and therefore erosion rates, that is especially strong in the north. This partially explains the spatial variation in the relative sensitivity of the north and south coastal sections to changes in wave direction.

6.2 Sand protection and the impact of increasing wave height

The spatial variation in erosion is important in demonstrating the morphological sensitivity of the Holderness coastline, as the majority of transported sediment is derived from the cliffs within the coastal domain. In the simulation, beach volume is spatially heterogeneous at any particular time, tending to reflect pulsed fluxes of sediment migrating in the southerly longshore drift direction. These flux pulses are relatively small in the north, where sediment input is limited. They increase in size towards the centre of the model, where they reach a maximum, migrating at around 1 km yr^{-1}. Although differing in shape, these pulses are analogous to the “ord” sandbars described and discussed by Pringle (1985), who related coastal erosion to ord movement. The movement of these sand bodies along the shoreface, integrated over the decadal to centennial scale, reduces erosion rates along the entire coast. The ords are formed under the current wave climate in the northern part of the coast, where the shadowing effect of Flamborough Head begins to diminish. Their formation in the northern region of the model is controlled by the driving wave climate. Changes in wave direction that modify wave-coastline angles to those more susceptible to sediment flux convergence (counter-clockwise) form the simulated ords earlier in their migration. These features protect the coastline over more northerly reaches than is currently the case under restricted wave climates.

Although not as strong, the relationship between increasing wave height and reduced erosion under rotated wave climates can also be explained by the pulsed fluxes of beach sediment and the protection that greater volumes of beach sand provide. As there is no influx of sediment around Flamborough Head, beach widths in the most northerly regions of the coast can not grow sufficiently to protect the soft-till cliffs from erosion. Increasing wave height laterally extends this zone of reduced beach protection by increasing the gradient in sediment transport, generating more sediment input from cliff retreat and increasing the availability of sand for beach protection further south. The reduction in erosion created by the added beach protection outweighs the increased erosion along the cliffs in the north, reducing overall erosion along the coast when wave height is increased.

6.3 Shadow zone

The final effect on variations in simulated erosion, results from the shadow zone caused by Flamborough Head. As the shoreline extends seawards to a salient (Flamborough Head), portions of the shoreline are shadowed to waves of particular orientations. At each time step in the model, the wave direction is determined and the shoreline scanned for shore segments that are shadowed. Wave height, and concurrently sediment transport, within the shadow is set to zero. This method assumes the salient is a prominent coastal feature and, therefore, wave energy retained for sediment transport following refraction is greatly reduced. Ashton and Murray (2006a) provide a detailed description of the shadow function with the CEM. The extent of the shadowed region changes with changing offshore wave direction at each time step. Due to the orientation of Flamborough Head, waves from the north create the largest shadow zone, while waves from the east and south no shadow zone. Thus, the area shadowed by the salient is progressively modified and with rotating wave climate sediment transport rates will be changed accordingly.

6.4 Caveats

Although the model produced a reasonable representation of erosion rates during calibration, it is important to highlight the caveats of using such a model for sensitivity analysis. The basis for many of these caveats surrounds the simplified representation of physical processes within the CEM.

The complete geometric shadowning assumed by the model on the downdrift side of a salient, forms a region in the model with no sediment transport processes. In reality, complex refraction, and diffraction, of the wave around the saleint would occur, sending a part of the wave energy into into the shadowed zone and modifying the approach angle of waves. However, the main effect of greatly reducing sediment transport within the shadow is captured.

As with the calibration, the geology within each erodible rock type for the transient simulation is assumed to be heterogeneous and free from any dominating, anisotropic features, such as rivers or major fractures. In addition to these assumptions, the transient simulations also assume that the eroding geology is homogeneous throughout. Smaller scale features are integrated implicitly by the calibration phase. However, larger features, such as the stream mouth north of Withernsea, will not be properly reflected by the simulation.

A future wave climate is unlikely to be similar to the simply perturbed current wave climate used in this study. It assumes that weather patterns are essentially the same as they were in 2009–10, and there has been no attempt to reflect possible changes in storminess. However, by using an ensemble approach, the range of likely effects on the morphological characters of the Holderness coastline is captured.

Predicted sea-level rise for the Holderness coast should not have a significant influence on wave climate, and the direct influence on coastal recession is thought to be quasi-linear. Thus, the simulation undertaken here does not include sea-level rise and our results need to be considered in conjunction with estimates of recession rates from such rises. Bray and Hooke (1997), suggested an increase in recession rates of between 22 % and 133 % by 2050 using a modified Brunn Rule method, while Castedo et al. (2012) used their cliff recession model to derive a linear increase in recession rates ranging from 0.015 $\mathrm{m\,yr^{-1}}$ for an annual sea level increases in of 1 mm to 0.32 $\mathrm{m\,yr^{-1}}$ for a annual sea level increase of 10 mm.

7 Conclusions and further work

An ensemble of 1350 simulations of coastal erosion were undertaken, each forced with a gradually perturbed version of the recorded wave climate to represent the period from 2010 to 2100. A baseline run was undertaken using the current wave climate from

2009–10 cycled over ninety years. This provided a baseline against which to examine the model runs using the stochastically varied wave climate.

Over the next ninety years to 2100, landward retreat remains close to zero for the chalk outcrop in the north which pins the system. Central to southern till sections exhibit the greatest sensitivity to wave climate. By summing the relative changes in erosion for each scenario, the individual influences of wave rotation and wave height can be assessed. Considering the Holderness coast as a whole, counter-clockwise rotation of the wave climate broadly reduces the rate of erosion, whilst clockwise rotations increase rates. Although the correlation is less strong, wave heights also have an impact on erosion; however, due to the protection provided by updrift stores of sediment, they unexpectedly lead to an average reduction in relative erosion with increasing height. Fundamental changes to the system do not occur in the first 40 yr of simulation, during which modifications to the wave climate are applied linearly.

The sensitivity of the coast to these changes in wave climate is spatially variable, with broadly differing impacts in the northern and southern regions. The combination of incident wave angle, wave shadowing and variable beach protection results in northern regions of the coast showing the greatest sensitivity to changes in wave climate. The range in absolute erosion by 2100 in this region is 60 m, or ±25 % relative to baseline at the 10th and 90th percentiles. Difference in the relative influences of perturbations in wave height and rotations of wave direction were also found for the northern and southern regions of the Holderness coast. These differences suggest that the northern region is more sensitive to changes in direction and the southern region to changes in the wave height and wave direction combined.

It is recognised that improvements to the prediction of coastal sensitivity for the Holderness coast would be possible through representation of coastal defence structures. These defences act as non-erodible surfaces, arresting the landward retreat of the coastline. Whilst effective where located, it is clear that these defences tend to increase erosion rates in adjacent sectors down the coast. Future research on soft-cliff, sandy coastlines, using the model presented here, will examine the impact of defensive struc-

Title Page
Abstract | Introduction
Conclusions | References
Tables | Figures
◂◂ | ▸▸
◂ | ▸
Back | Close
Full Screen / Esc
Printer-friendly Version
Interactive Discussion

tures along the coast on mesoscale erosion rates. Recession rates will be extrapolated into the future under a set of changing wave climate conditions similar to this study. We will then use similar wave climate perturbations to simulate the interactions between these and coastal defences, and concurrent impact on the erosion of adjacent sectors of coastline. Further improvements to the model will incorporate: the influence of sea-level rise on recession rates, for use where a non-linear influence on coastal erosion is expected; and a better representation of future wave climate scenarios that include, for example, the role of increasing storm frequency on recession rates.

Acknowledgements. The authors are grateful to Martin Hurst of the British Geological Survey for reviewing this paper and returning feedback that lead to its improvement. This paper is published with the permission of the Executive Director of the British Geological Survey (NERC), and was supported by the Climate and Landscape research programme at the BGS.

References

Adams, P. N., Anderson, R. S., and Revenaugh, J.: Microseismic measurement of wave energy delivery to a rocky coast, Geology, 30, 895–898, 2002.

Ashton, A., Murray, A. B., and Arnoult, O.: Formation of coastline features by large-scale instabilities induced by high-angle waves, Nature, 414, 296–300, 2001.

Ashton, A. and Murray, A. B.: High-angle wave instability and emergent shoreline shapes: 1. Modeling of sand waves, flying spits, and capes, J. Geophys. Res.-Surf., 111, F04011, doi:10.1029/2005JF000422, 2006a.

Ashton, A. and Murray, A. B.: High-angle wave instability and emergent shoreline shapes: 2. Wave climate analysis and comparisons to nature, J. Geophys. Res. Earth Surf., 111, F04012, doi:10.1029/2005JF000423, 2006b.

Bladé, I., Liebmann, B., Fortuny, D., and van Oldenborgh, G. J.: Observed and simulated impacts of the summer NAO in Europe: implications for projected drying in the Mediterranean region, Clim. Dynam., 39, 709–727, 2012.

Bray, M. J., Hooke, J. M.: Prediction of soft-cliff retreat with accelerating sea-level Rise, J. Coastal Res., 13, 453–467, 1997.

Brown, S., Barton, M. E., and Nicholls, R. J.: The effect of coastal defences on cliff top retreat along the Holderness coastline, P. Yorks. Geol. Soc., 59, 1–13, 2012.

Castedo, R., Murphy, W., Lawrence, J., and Paredes, C.: A new process–response coastal recession model of soft rock cliffs, Geomorphology, 177–178, 128–143, 2012.

Catt, J. A.: The Pleistocene glaciation of eastern Yorkshire: a review, P. Yorks. Geol. Soc., 56, 177–207, 2007.

CCO: Channel Coastal Observatory, http://www.channelcoast.org/data_management/real_time_data/charts/?chart=72, last access: July 2013.

Ciavola, P.: Coastal dynamics and impact of coastal protection works on the Spurn Head spit (UK), Catena, 30, 369–389, 1997.

Clark, H. C. and Johnson, M. E.: Coastal Geomorphology of Andesite from the Cretaceous Alisitos Formation in Baja California (Mexico), J. Coastal Res., 11, 401–414, 1995.

de Boer, G.: Spurn Head: its history and evolution, T. I. Brit. Geogr., 34, 71–89, 1964.

DEFRA: Charting Progress 2. Feeder Report: Ocean Processes, Department for Environment Food and Rural Affairs, on behalf of the UK Marine Monitoring and Assessment Strategy community, Department for Environment Food and Rural Affairs on behalf of the UK Marine Monitoring and Assessment Strategy community, Nobel House, London, UK, 2010.

Dickson, M. E., Kennedy, D. M., and Woodroffe, C. D.: The influence of rock resistance on coastal morphology around Lord Howe Island, southwest Pacific, Earth Surf. Proc. Land., 29, 629–643, 2004.

Gibbons, C. R.: A study of the different types of landslides and the associated rates of recession along the Holderness coast, East Yorkshire, MSc thesis, University of Leeds, 2004.

Grabemann, I. and Weisse, R.: Climate change impact on extreme wave conditions in the North Sea: an ensemble study, Ocean Dynam., 58, 199–212, 2008.

Hapke, C. and Reid, D.: National assessment of shoreline change, Part 4: Historical coastal cliff retreat along the California coast, US Geological Survey Open-file Report, 2007–1133, 1–51, 2007.

Hulme, M., Jenkins, G., Lu, X., Turnpenny, J., Mitchell, T., Jones, R., Lowe, J., Murphy, J., Hassell, D., Boorman, P., Macdonald, R., and Hill, S.: Climate-Change Scenarios for the UK: The UKCIP02 Scientific Report, Tyndall Centre for Climate Change Research, 2002.

Hurrell, J. W.: Decadal trends in the North-Atlantic Oscillation – Regional temperatures and precipitation, Science, 292, 676–679, 1995.

Hurrell, J. W. and van Loon, H.: Decadal variations in climate associated with the North Atlantic Oscillation, Climate Change, 36, 301–326, 1997.

IECS: Humber Estuary and Coast, Institute of Estuarine and Coastal Studies, University of Hull, Hull, UK, 1994.

IPCC: Climate Change 2007: vol 4, Cambridge University Press, Cambridge, UK, 2007.

Komar, P. D.: The mechanics of sand transport on beaches, J. Geophys. Res., 76, 713–721, 1971.

Lee, E. M.: Coastal cliff behaviour: observations on the relationship between beach levels and recession rates, Geomorphology, 101, 558–571, 2008.

Limber, P. W. and Murray, A. B.: Initial modeling of rocky coastline responses to reductions in fluvial sediment supply, Proceedings of the 7th IAHR Symposium on River, Coastal, and Estuarine Morphodynamics, Beijing, China, 2011a.

Limber, P. W. and Murray, A. B.: Beach and sea cliff dynamics as a driver of rocky coastline evolution and stability, Geology, 39, 1149–1152, 2011b.

Limber, P. W., Patsch, K. B., and Griggs, G. B.: Coastal sediment budgets and the littoral cut-off diameter: a grain-size threshold for quantifying active sediment inputs, J. Coastal Res., 24, 122–133, 2008.

List, J., Farris, A. H., and Sullivan, C.: Reversing storm hotspots on sandy beaches: spatial and temporal characteristics, Mar. Geol., 226, 261–279, 2006.

List, J. H. and Ashton, A. D.: A circulation modeling approach for evaluating the conditions for shoreline instabilities, Coastal Sediments 2007, 327–340, Am. Soc. of Civ. Eng., Reston, Va, 2007.

May, V. J.: Flamborough Head, Volume 28: Coastal Geomorphology of Great Britain Chapter 4: Soft-rock cliffs – GCR site reports, J S Publications, Suffolk, UK, 1980.

McNamara, D., Murray, A. B., and Smith, M. D.: Coastal sustainability depends on how economic and coastline responses to climate change affect each other, Geophys. Res. Lett., 38, L07401, doi:10.1029/2011GL047207, 2011.

Metropolis, N. and Ulam, S.: The Monte Carlo method, J. Am. Stat. Assoc., 44, 335–341, 1949.

Montreuil, A.-L. and Bullard, J. E.: A 150 yr record of coastline dynamics within a sediment cell: Eastern England, Geomorphology, 179, 168–185, 2012.

Newsham, R., Balson, P. S., Tragheim, D. G., and Denniss, A. M.: Determination and prediction of sediment fields from recession of the Holderness Coast, NE England, J. Coastal Conserv., 8, 49–54, 2002.

Pendleton, L. H.: The economic and market value of coasts and estuaries: what's at stake? Coastal Ocean Values Press, Washington DC, USA, 2010.

Perg, L. A., Anderson, R. S., and Finkel, R. C.: Use of cosmogenic radionuclides as a sediment tracer in the Santa Cruz littoral cell, California, United States, Geology, 31, 299–302, 2003.

Pringle, A. W.: Holderness coast erosion and the significance of ords, Earth Surf. Proc. Land., 10, 107–124, 1985.

Quinn, J. D., Philip, L. K., and Murphy, W.: Understanding the recession of the Holderness Coast east Yorkshire, UK: a new presentation of temporal and spatial patterns, Q. J. Eng. Geol., and Hydroge., 42, 165–178, 2009.

Quinn, J. D., Rosser, N. J., Murphy, W., and Lawrence, J. A.: Identifying the behavioural characteristics of clay cliffs using intensive monitoring and geotechnical numerical modelling, Geomorphology, 120, 107–122, 2010.

Robert, C. P. and Casella, G.: Monte Carlo Statistical Methods, Secaucus, NJ, USA: Springer, New York, Inc., 2 edn., 2004.

Robertson, I.: Erosion and Stability of Till Cliffs on the Holderness Coast, Ph.D. Thesis, University of Newcastle Upon Tyne, University of Newcastle Upon Tyne, Newcastle, UK, 1990.

Sallenger, A. H., Krabill, W., Brock, J., Swift, R., Manizade, S., and Stockdon, H.: Seacliff erosion as a function of beach changes and extreme wave runup during the 1997–1998 El Nino, Mar. Geol., 187, 279–297, 2002.

Scott Wilson: Humber Estuary Coastal Authorities Group (HECAG), Flamborough Head to Gibraltar Point Shoreline Management Plan 2, Scott Wilson, Basingstoke, Hampshire, UK, 2009.

Slott, J. M., Murray, A. B., Ashton, A. D., and Crowley, T. J.: Coastline responces to changing storm patterns, Geophys. Res. Lett., 33, L18404, doi:10.1029/2006GL027445, 2016.

Sutherland, J. S. and Wolf, J.: Coastal defence vulnerability 2075, HR Wallingford Report SR590, H R Wallingford, Wallingford, UK, 2002.

Thornton, E. B., Sallenger, A., Conforto, S. J., Egley, L., McGee, T., and Parsons, R.: Sand mining impacts on long-term dune erosion in southern Monterey Bay, Mar. Geol., 229, 45–58, 2006.

Trenhaile, A. S., Pepper, D. A., Trenhaile, R. W., and Dalimonte, M.: Stacks and notches at Hopewell Rocks, New Brunswick, Canada, Earth Surf. Proc. Land., 23, 975–988, 1998.

Valentin, H.: Land Loss at Holderness, Applied Coastal Geomorphology, edited by: Steers J. A., 116–137, Macmillan, 1971.

Valvo, L., Murray, A. B., and Ashton, A.: How does underlying geology affect coastline change? An initial modeling investigation, J.Geophys Res. Ea. Surf., 111, F02025, doi:10.1029/2005JF000340, 2006.

van den Berg, N., Falqués, A., and Ribas, F.: Modeling large scale shoreline sand waves under oblique wave incidence, J. Geophys Res. Ea. Surf., 117, F03019, doi:10.1029/2011JF002177, 2012.

Wang, X. L., Zwiers, F. W., and Swail, V. R.: North Atlantic Ocean Wave Climate Change Scenarios for the Twenty-First Century, J. Climate, 17, 2368–2383, 2004.

Walkden, M. J. A. and Hall, J. W.: A predictive mesoscale model of the erosion and profile development of soft rock shores, Coast. Eng., 52, 535–563, 2005.

Woollings, T.: Dynamical influences on European climate: an uncertain future, Philos. T. Roy. Soc. A, 368, 3733–3756, 2010.

Woollings, T., Hannachi, A., Hoskins, B., and Turner, A.: A regime view of the North Atlantic Oscillation and its response to anthropogenic forcing, J. Climate, 23, 1291–1307, 2010.

Woth, K., Weisse, R., and von Storch, H.: Climate change and North Sea storm surge extremes: an ensemble study of storm surge extremes expected in a changed climate projected by four different regional climate models, Clim. Dynam., 26, 3–15, 2006.

Young, A. P. and Ashford, S. A.: Instability investigation of cantilevered seacliffs, Earth Surf. Proc. Land., 33, 1661–1677, 2008.

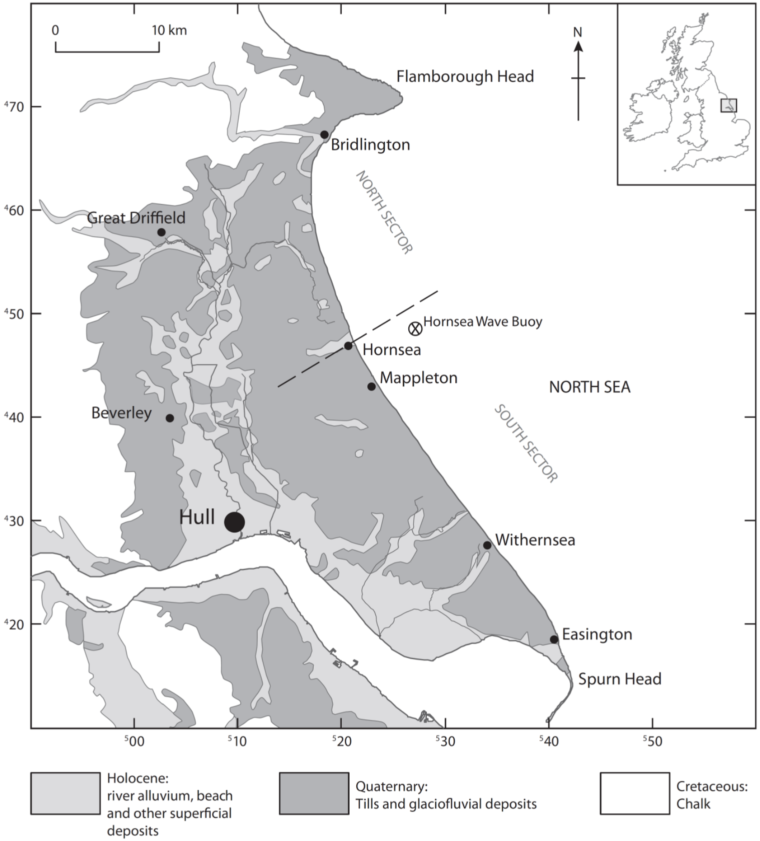

Fig. 1. Geological composition of the Holderness coast (main) and the location of the region within the UK (insert). Also indicated are the positions of the Hornsea wave buoy, from which wave climate was recorded, and the division into northern and southern coastline regions, as referenced by the sea wall at Hornsea (dashed line), to aid analysis.

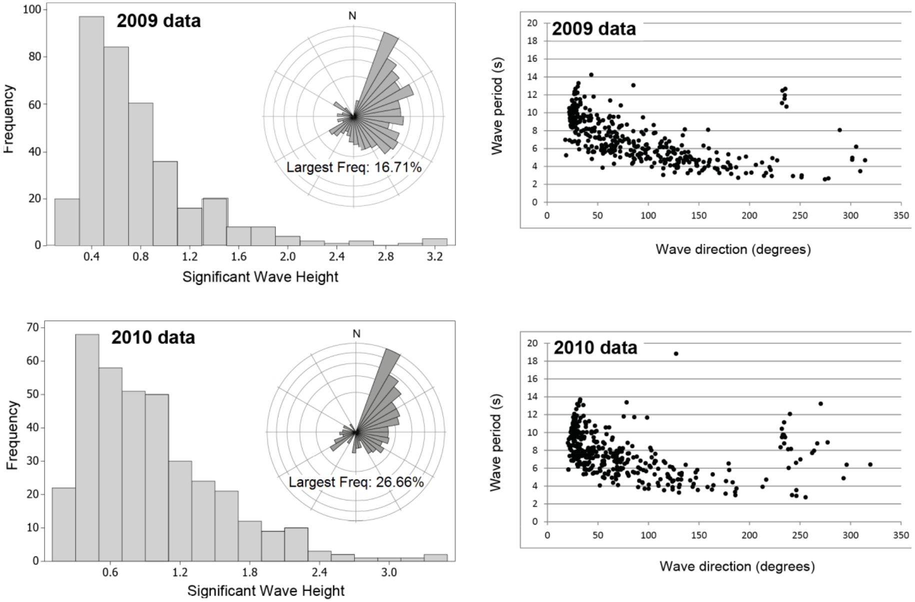

Fig. 2. Wave climates used in the modelling. The data are daily averages, calculated from the data recorded every 30 min by the Hornsea WaveRider III buoy (CCO, 2013). The rose diagrams show the direction from which the wave is travelling. The "petals" are in 10° intervals and area-scaled by frequency percent. The dominance of waves travelling from northeasterly directions is clear, particularly during 2010. Note the low frequencies of waves travelling in offshore directions.The histograms show that significant wave height data are positively skewed, but with marked variations in height frequencies over each year. Neither are well-fitted to standard distributions, either in raw or transformed form. Overall, there were greater frequencies of higher waves in 2010, suggesting more unsettled weather than in 2009. *N* = 365 in both roses and histograms.

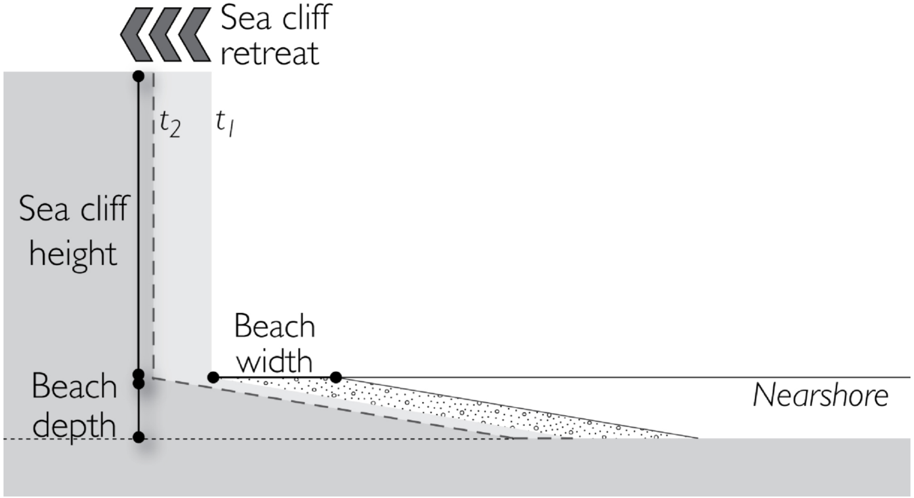

Fig. 3. Cross sectional view of the shoreface and cliff retreat variables, as defined for the modified coastal evolution model used in this study.

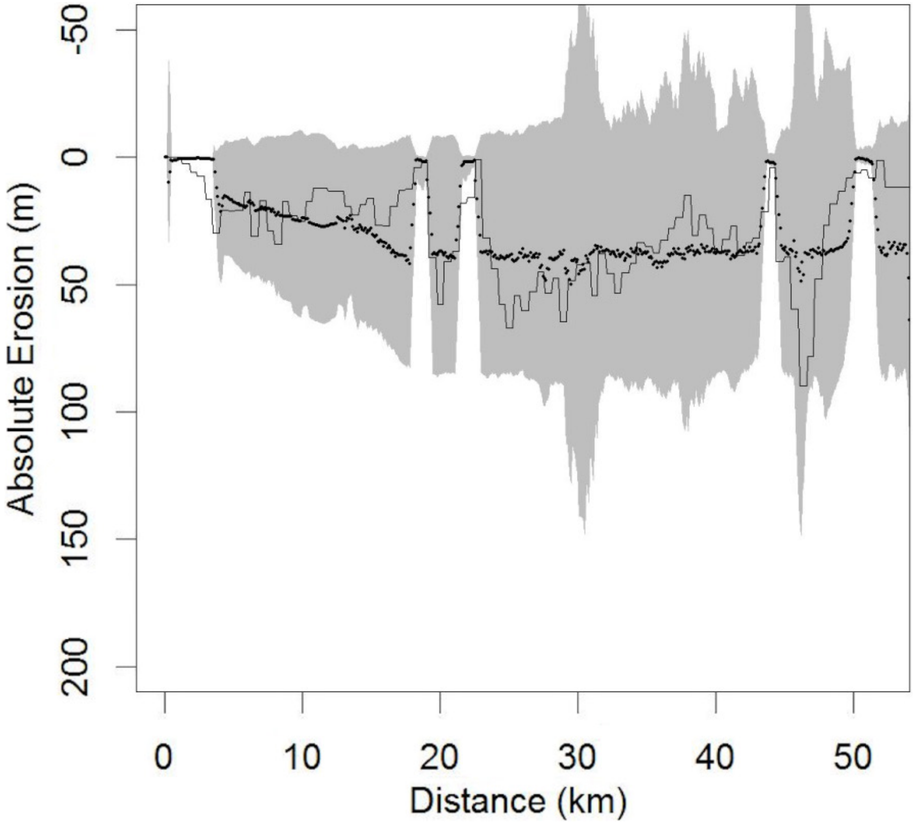

Fig. 4. Range of simulated coastline retreat over a 15 yr period, as captured during the ensemble calibration process (grey shadowing). The observed rates of change between 1995 and 2010 (modified from Montreuil and Bullard, 2012) are given as the solid black line and the ensemble member with the lowest RMSE plotted as a series of points for comparison.

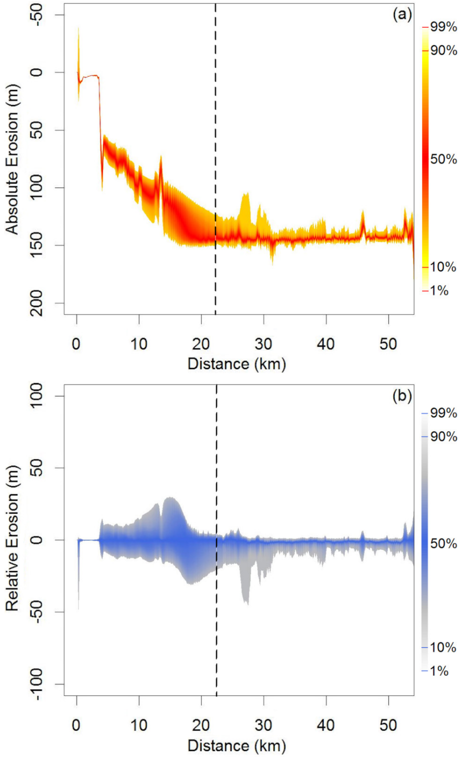

Fig. 5. Simulated absolute change in coastline position **(a)** from 2010 to 2100 predicted using an ensemble of future wave climates. Relative change in coastline position **(b)**, as referenced to the baseline for each member of the ensemble. The range of colours in each plot represents the ensemble percentiles as given on the right of the figures. The black dashed line represents the divide between the northern region (to the left) and the southern region (to the right) as defined in the text.

Title Page
Abstract Introduction
Conclusions References
Tables Figures
◄◄ ►►
◄ ►
Back Close
Full Screen / Esc
Printer-friendly Version
Interactive Discussion

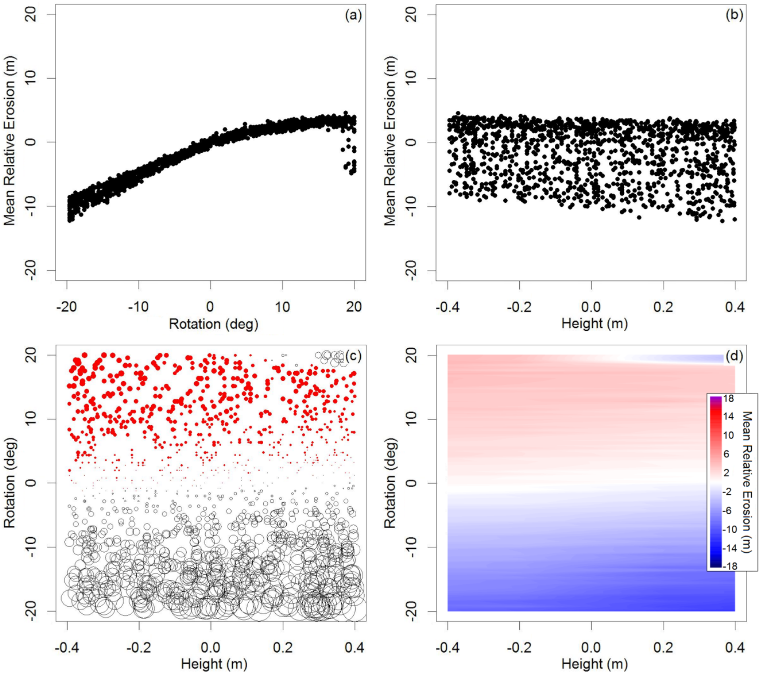

Fig. 6. Wave rotation **(a)** and wave height **(b)** components of wave climate plotted against spatially averaged mean relative erosion over the ninety year period. Negative erosion values indicate a relative reduction in the erosion rate in comparison to the baseline. Wave height and rotation perturbation factors are plotted together **(c)**. The size of each symbol is relative to the change in mean erosion rate imparted by that wave climate in comparison to the baseline scenario. Red dots represent increased erosion relative to the baseline and empty circles reduced erosion. The same data have been a contoured **(d)**. The scale on this plot represents spatially averaged (mean value for the coast as a whole) relative erosion (m) after ninety years of simulation.

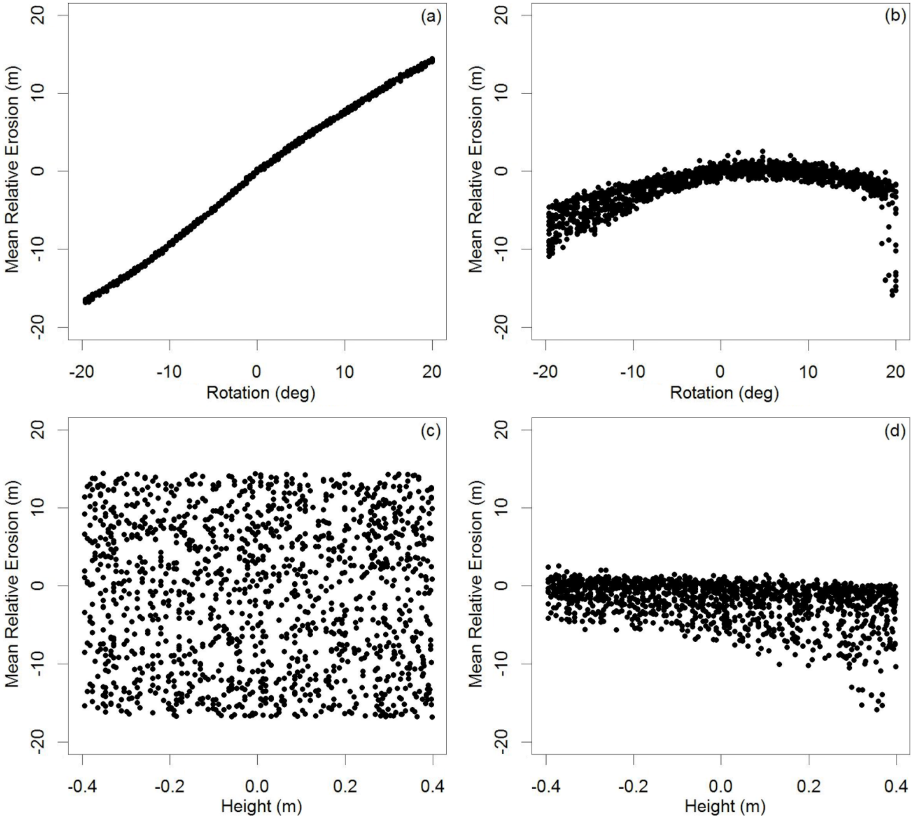

Fig. 7. Wave rotation perturbation plotted against spatially averaged mean relative erosion for the north **(a)** and south **(b)**. Negative values indicate a reduction in the erosion rate. Wave height perturbations are also plotted against spatially averaged mean relative erosion for the north **(c)** and south **(d)**.

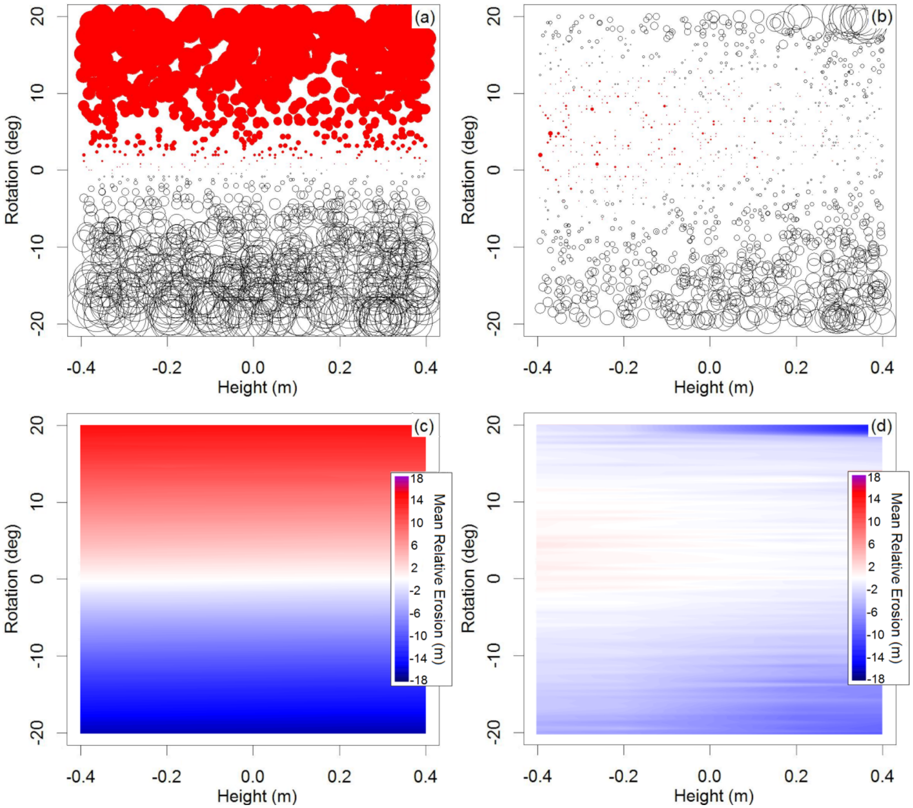

Fig. 8. Wave height and rotation perturbation factors are plotted against each other for the north **(a)** and south **(b)** of the model domain. The size of each symbol is relative to the change in mean erosion rate imparted by that wave climate in comparison to the baseline scenario. Red dots represent increased erosion relative to the baseline and empty circles reduced erosion. Interpolated contour plot of the height change component of wave climate against the wave rotation component for the north **(c)** and south **(d)** of the model domain are also given.

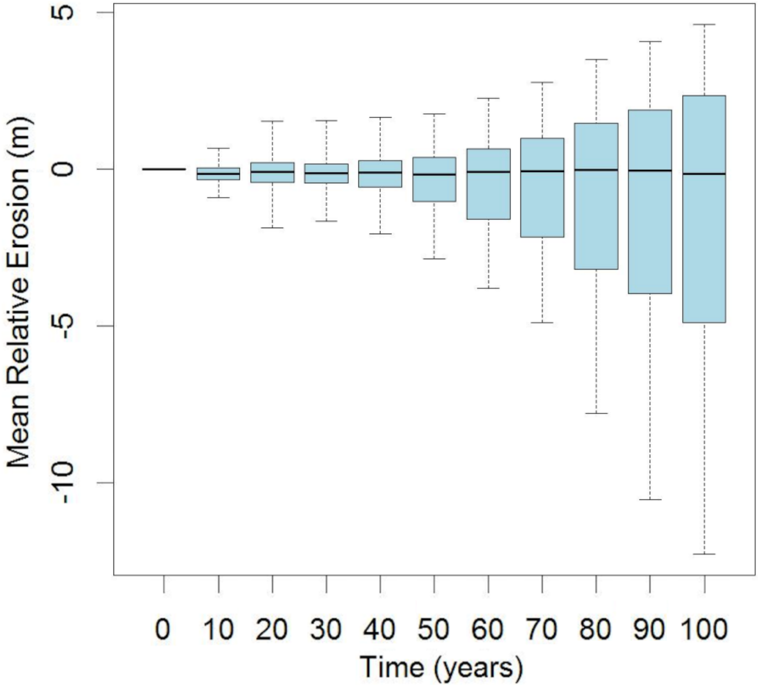

Fig. 9. Box and whisker plot showing the evolution of spatially averaged mean relative coastal erosion, in comparison to the baseline, through time. The central bars represent the median value, the blue boxes show the interquartile range and the extended bars represent extreme values.